Evolution and interaction of surface cracks under thermal shock load

Xiaosong Wang*, Weizheng Zhang**
*Beijing Institute of Technology, Beijing 100081, China, E-mail: 3120120232@bit.edu.cn
**Beijing Institute of Technology, Beijing 100081, China, E-mail: xiaomibide@126.com

1. Introduction

The thermal shock/fatigue problem is increasingly notable on the reliability of structure and material in modern engineering fields, such as vehicle industry, nuclear industry and surface technics. It is generally believed that under the thermal shock/fatigue load, thermal cracks would nucleate on the surface of the material and cause thermal fatigue failure through crack propagation. Researchers have found that the initiation of thermal cracks is multi-sourced, and thermal fatigue crack network is the typical crack morphology caused by cyclic thermal load [1-3].

In the past few years, thermal crack problem has drawn much attention of researchers. Maillot et al [1] conducted a thermal fatigue test and studied the crack network parameters experimentally. It indicated that the crack network would stabilize with the cycles. A computational study of this thermal crack network was also presented by Haddar [4]. By applying thermal shock heat flux on the finite element model, the thermal shock temperature and thermal stress field were evaluated. The growth of the crack network was also predicted by considering the shielding effects. Kamaya et al [5] examined the mechanism of the evolution of crack network and its influences on crack growth by numerical calculation under thermal fatigue load. It was found that the interaction between cracks affected the initiation rather than the growth of cracks. Moreover, the crack network appears only when the crack growth in the depth direction was interrupted.

As a common parameter to character the ability of crack propagation, the stress intensity factor (SIF) is widely used in investigating the interactions among multi-cracks. Tsang et al [6] investigated the SIF of parallel penny-shaped cracks under *I*-type load. The results showed that the SIF of the inner crack was lower than a single crack by 16% to 48%, and the outer crack had the highest SIF and was most likely to fail. Kamaya [7, 8] evaluated the growth behaviour and the SIF of interacted coplanar and parallel semi-elliptical surface cracks through finite element analysis quantitatively. Lam et al [9] studied the effect on the SIF of plane strain multi-cracks and found that the interactions between cracks could produce either enhancing or shielding effect on SIF depending on the positions and orientations of the cracks. Bouiadjra et al [10] investigated the plastic strain ahead of main crack with different dispositions of microcracks. It was found that the effect of the micro-cracks disappeared when the relative distance was greater than 10%.

The main objective of this paper is to investigate the evolution and interaction of surface thermal cracks under thermal shock load. The thermal shock test is conducted to study the temperature distribution and thermal crack behaviour. Then crack models are established through finite element method (FEM) to investigate the temperature, thermal stress and SIF distributions along crack tips under thermal shock load. Furthermore, the evolution of thermal cracks in experiment is also analysed combined with the FEM results qualitatively.

2. Experimental procedures and results

The thermal shock test is carried out through the high-frequency induction heating device, in which the specimens are alternately heated by induction coil and cooled by water quenching [2]. A whole thermal shock cycle includes heating up to highest temperature in 60 s and cooling down to room temperature in 15 s. During the test, the specimens are free from any external load and constraint, so the initiation of the thermal cracks are totally caused by the thermal load. The specimens are cylindrical and made of compacted graphite iron, with the diameter of 30mm and thickness of 10 mm. Thermocouples were arranged on the specimen surface to monitor the temperature distributions. Before the test, the specimens need to be polished to remove the surface irregularities and notches. During the intervals of the thermal cycles, the optical microscope (PTI-1800) is used to observe and record the thermal cracks morphology on the specimen surface.
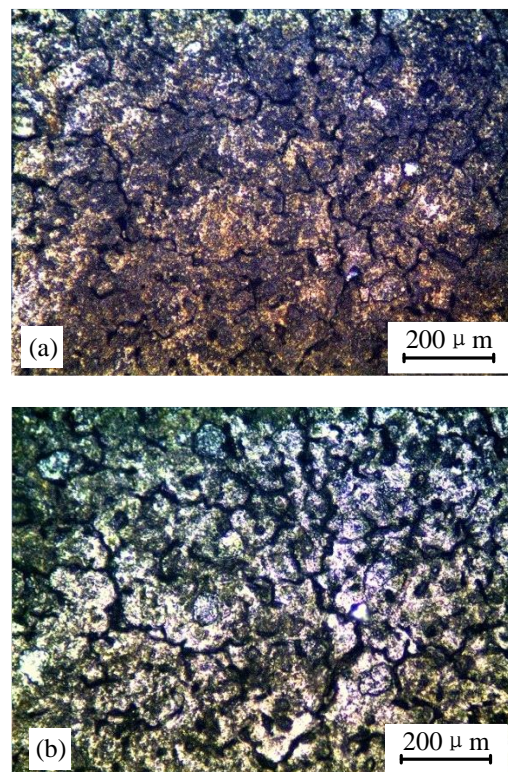

Fig. 1 Evolution of surface thermal cracks, no polishing:
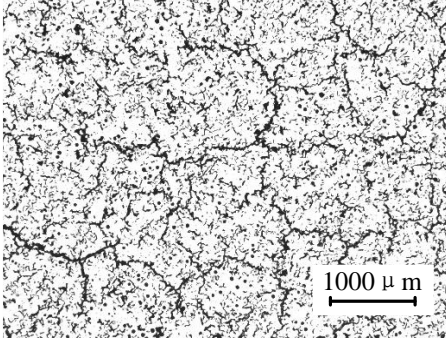a - 50 cycles; b - 100 cycles

Fig. 2 Thermal crack network, after surface polishing

3. FEM models

The widely used commercial finite element software ABAQUS is applied to investigate the temperature, thermal stress and SIF distribution in crack models under thermal shock load. Assume that the surface crack is semicircular, with the average crack length of $2a = 1$ mm. Parallel and coplanar cracks distribution are considered in this paper and the distributions are illustrated in Fig. 3, where a and Φ correspond to the crack angle and crack length, and the parameters d and l denote the distance between parallel and coplanar cracks, respectively. In this paper, the crack spacing ratio (d/a and l/a) changes in the range of 0 ~ 4, and the size of FEM models is much larger than the crack size.
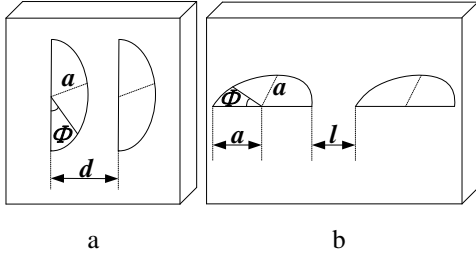

Fig. 3 Distributions of parallel (a) and coplanar (b) cracks

The degenerated 20-node iso-parametric elements are used in the crack models to eliminate the $r^{-1/2}$ singularity in I-type crack tips. In this element, one surface of the traditional 20-node iso-parametric elements degenerated into an edge, then the mid-nodes of the adjacent edges move to the 1/4 position, as shown in Fig. 4. The gridding around the crack tips are shown in Fig. 5, where the sur

face OABO' donates the crack surface, and the points O and O' correspond to the crack tips on the heating surface and in the depth direction. Frictionless contact interaction is set for the crack surfaces. According to the thermal shock test, no external load or constraint is applied.
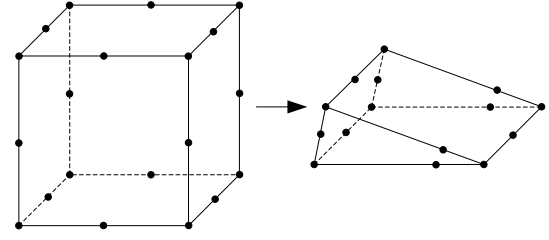

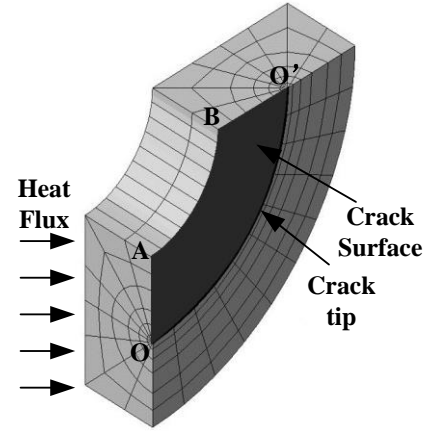Fig. 4 Degenerated 20-node iso-parametric element

Fig. 5 Gridding around the crack tip

Considering that the simulation of induction heating is complex and costly, the constant heat flux is used to replace the induction heating during the simulating. In the cooling process, surface heat transfer is set to simulate the water quenching process in real test.

In ABAQUS, the J-integral in crack model is calculated through a cannular area enclosing the crack tips. And the SIF along the crack tips can be estimated in

$$K_I = \left(\frac{8\mu J}{1+\kappa} \right)^{1/2}, \tag{1}$$

where the parameter $\kappa = (3-v)/(1-v)$ in plane stress condition and $\kappa = 3-4v$ in plane strain and 3D condition.

Table
Comparison of SIF (normalized) with Raju-Newman's work

$2\Phi/\pi$	0	0.125	0.25	0.375	0.5	0.625	0.75	0.875	1
Present	1.201	1.152	1.110	1.087	1.072	1.063	1.057	1.054	1.053
Raju-Newman [11]	1.174	1.145	1.105	1.082	1.067	1.058	1.053	1.050	1.049
Relative error (%)	2.25	0.65	0.47	0.46	0.50	0.46	0.39	0.38	0.38

4. FEM results

4.1. Model validation

To verify the validity and reliability of the established FEM model, the simulation results of the SIF along the crack tips are compared with Raju-Newman's research

[11]. Table gives the comparison of the SIF in different crack angles. It shows that the calculated SIF in the present model are highly consistent with Raju-Newman's work, and the maximal discrepancy of the SIF is less than 3%. So, the established FEM crack model in this paper is effective and credible in calculating and investigating the interactions between thermal cracks.

4.2. Temperature

During the thermal shock test, the thermal stress in the structure is caused by the temperature gradient in the depth direction of the specimen. So it is of great importance to simulate the model temperature field accurately. By modifying the amplitude of heat flux, the simulated temperature gradient agrees well with the temperature measured during the test. Fig. 6 gives the comparison of the model and test temperature of the heating surface and bottom surface. Because of the hysteresis of heat conduction, the temperature gradient always exists during the whole thermal cycle between different specimen surfaces. Thus, the thermal stress would be caused in the depth direction, especially in the cooling process, where the largest temperature gradient is occurred.
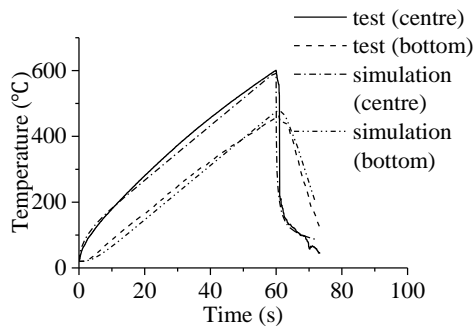

Fig. 6 Temperature curves

4.3. Thermal stress

Thermal damages initiate form the specimen surface. Fig. 7 gives the thermal stress caused in the specimen surface under thermal shock load. It shows that thermal stress exists in the whole process. In the heating process, the temperature rises and a stable temperature discrepancy is caused in the depth direction, leading to a surface compressive thermal stress. However, in the cooling process, the temperature of heating surface drops rapidly but the bottom surface remains in high temperature due to the hysteresis of heat conduction. In this circumstance, a large instantaneous tensile thermal stress is occurred on the surface and then it drops with the decreasing of temperature gradient. The instantaneous maximal tensile thermal stress value would reach about 400 MPa, which exceeds the yielding stress of the material and would probably lead to the thermal damage on the material surface.
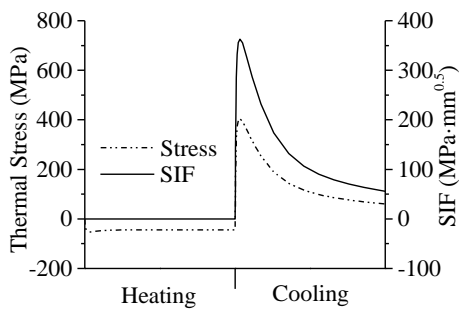

Fig. 7 Thermal stress and SIF in thermal cycles

Fig. 8 presents the distribution of thermal stress component σ_{xx} along the depth direction under maximal surface stress. It shows that the large tensile thermal stress is formed in a thin layer of the heating surface, which proves that the nucleation, propagation and coalescence of thermal cracks would only occur and be promoted on the specimen surface. Moreover, the thermal stress would turn into compressive stress with the depth increasing, which would also inhibit the crack propagation along the depth direction.

Furthermore, the cooling speed of the specimen surface could also affect the amplitude of the surface thermal stress. The comparison of different cooling speeds in Fig.8 shows that the maximal instantaneous tensile thermal stress increases significantly with the cooling speed. However, little difference is found in the ranges of tensile thermal stress in different cooling speeds.
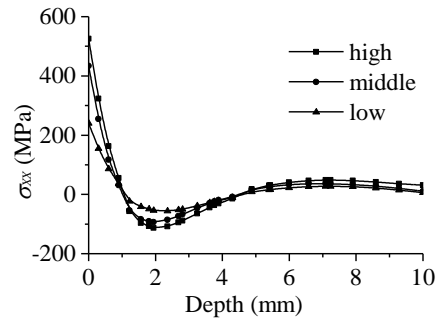

Fig. 8 σ_{xx} along depth direction in different cooling speeds

4.4. Single cracks

The thermal expansion effect leads to the closure of crack surface in the heating process, so the SIF remains zero. However, the crack surface would open and the SIF at surface crack tip would increase with the tensile thermal stress during the cooling process, as shown in Fig. 7.

Under the thermal shock load, the SIF along the surface crack tips show great difference with uniaxial tension. Fig. 9 gives the comparison of simulated SIF of these two loads. Due to the large thermal stress gradient in the depth direction (as shown in Fig. 8), the SIF show a notable decrease in the depth direction. It also indicates that the propagation of thermal crack along the depth direction is restricted, and the thermal cracks evaluation mainly occurs on the specimen surface.
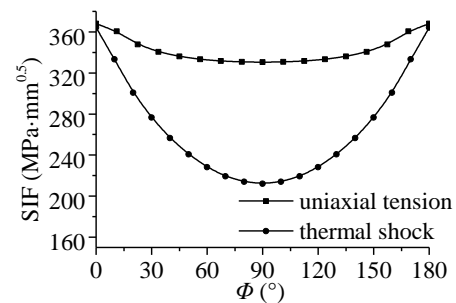

Fig. 9 Comparison of SIF

4.5. Double cracks

Parallel and coplanar cracks are considered to investigate the interaction of thermal cracks. Generally, parallel cracks present a shielding effect between each cracks owing to the same crack propagation directions, which would reduce the crack propagation ability of each other. However,

coplanar cracks reflect an enhancing effect due to the opposite crack propagation directions, which would promote the propagation and coalescence of each cracks.

4.5.1. Parallel cracks

The crack spacing ratio (d/a) has an important influence on the SIF in parallel cracks. Fig. 10 gives the SIF in parallel cracks with different d/a ratios. It shows that in small d/a ratio, the shielding effect is more notable. And with the increasing of d/a ratio, the SIF along crack tips increase and tend to be the values of single crack. It could be deduced that the shielding effect disappears when $d/a > 4$ in parallel cracks.
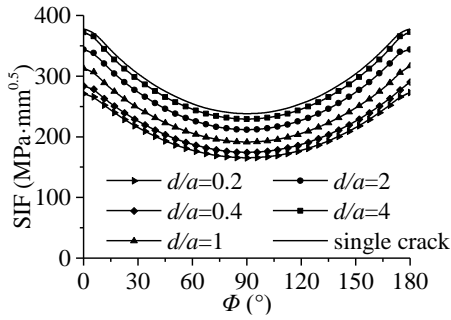

Fig. 10 SIF in parallel cracks

Define the crack shielding factor between parallel cracks as

$$k_p = K_{I,double} / K_{I,single} , \qquad (2)$$

where k_p donates the crack shielding factor; $K_{I,double}$ is the SIF in parallel cracks; $K_{I,single}$ is the SIF in single crack. The lower the k_p, the stronger the crack shielding effect in parallel cracks.

The relation between k_p and the d/a ratio is presented in Fig. 11. Besides, the results in the uniaxial tension [12], thermal shock load with external constraint and thermal conduction with external constraint [3] are also exhibited as comparison. It reveals that the external constraint could significantly enhance the crack shielding effect, inhibit the initiation and propagation of other cracks in a larger range, and promote the formation of local long cracks. However, the crack shielding effect under free condition is quite small. It is partly proved that the thermal crack network would develop on the specimen surface in this thermal shock test. But in real structure, long or main crack would easily nucleate, because of the large external constraint on thermal expansion effect.
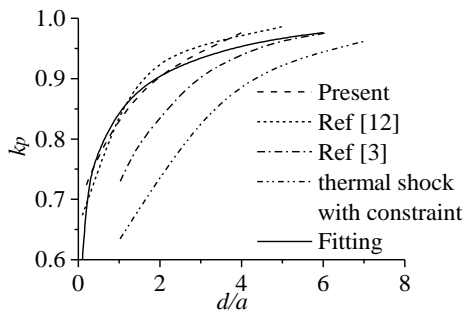

Fig. 11 Crack shielding factor in parallel cracks

Assume that k_p increases with the d/a ratio exponentially. So k_p could be drawn as

$$k_p = 1 - m\,e^{-nx_p^t} , \qquad (3)$$

where x_p donates the d/a ratio; m, n and t are the model parameters. When $x_p = 0$, it can be considered that the parallel cracks overlap, that is, $m = 0.5$. Fit the model parameters in Matlab program, and it is obtained that $n = 1.221$, $t = 0.511$. The fitting curve is also given in Fig. 11, and it agrees well with the FEM results.

4.5.2. Coplanar cracks

Fig. 12 shows the SIF in coplanar cracks at different l/a ratios. It reveals that only the inner crack tips reflect the notable enhancing in SIF, and the closer the inner crack tips the more notable the enhancing effect. So it could be deduced that the crack coalescence is prior than the crack propagation of surface crack, and the crack propagation in the depth direction is also inhibited.
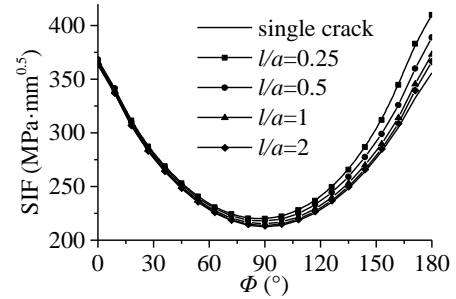

Fig. 12 SIF in coplanar cracks

Following the definition of crack shielding factor, define the crack enhancing factor between coplanar cracks as:

$$k_c = K_{I,double} / K_{I,single} , \qquad (4)$$

where k_c donates the crack enhancing factor.

Fig. 13 gives the relation between k_c and the l/a ratio at inner, depth and outer crack tips. Besides, the result of uniaxial tension [12] is also drawn in Fig. 13 as comparison. It shows that under thermal shock load the enhancing rates in depth and outer crack tips are both less than 3%. However, the enhancing effect of penetrated crack tips is significantly stronger than that of the coplanar cracks, which indicates that the surface thermal cracks would not propagate or coalescence into main cracks easily.
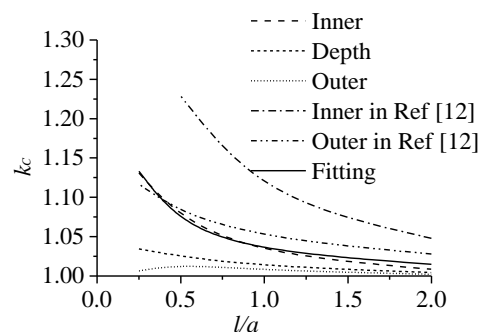

Fig. 13 Crack enhancing factor in coplanar cracks

Assume that when $l/a = 0$, the k_c of inner crack tips tend to be infinite. So that k_c could be satisfied with:

$$k_c = qx_c^p + 1, \qquad (5)$$

where x_c donates the l/a ratio; p and q are the model parameters. Fit the model parameters and it is obtained that $p = 0.031$, $q = -1.055$. The fitting curve is also given in Fig. 13, and it shows highly consistent with the FEM results.

5. Discussion

Test results show that the initiated thermal cracks finally form into surface thermal crack network. However, the thermal cracks propagation or growth in the depth direction seems to be negative.

Equally, through the FEM simulation, the thermal stress distribution reflects significant stress gradient along the depth direction. It indicates that the propagation of thermal cracks along the depth direction is inhibited. Furthermore, weak shielding and enhancing effect between thermal cracks are caused in parallel and coplanar cracks under thermal shock load without external constraint. All these effects reveal that large numbers of thermal cracks would nucleate on the material surface and the propagation ability of thermal cracks is low for both material surface and depth direction. Thus, the formation of surface thermal crack network on the material surface under thermal shock load is reasonable and inevitable.

6. Conclusions

Through the results of the thermal shock test and FEM simulation, the main conclusions of this paper could be drawn as follows

1. Under thermal shock load, thermal cracks nucleate at the graphite phases on the specimen surface largely. The initiated thermal cracks could connect with each other and gradually form in a stable thermal crack network.

2. A large instantaneous thermal stress and high stress gradient would occur on the heating surface during the cooling process. And the maximum tensile thermal stress increases with the cooling speed.

3. Thermal cracks exhibit low crack propagation ability along the depth direction. And the parallel and coplanar cracks also reveal quite weak interactions in crack shielding and enhancing effect compared with the restrained thermal cracks and penetrated cracks under uniaxial tension.

4. The simulation results prove that the formation of the thermal crack network is reasonable and it agrees well with the test results.

References

1. **Maillot, V; Fissolo, A; Degallaix, G; Degallaix, S.** 2005. Thermal fatigue crack networks parameters and stability: an experimental study, International Journal of Solids and Structure 42(2): 759-769.
http://dx.doi.org/10.1016/j.ijsolstr.2004.06.032.

2. **Wang, X; Zhang, W; Guo, B; Zhao, W.** 2014. The characteristics of microcrack initiation process in cast iron materials under thermal shock test, Materials Science and Engineering A 609(27): 310-317.
http://dx.doi.org/10.1016/j.msea.2014.05.012.

3. **Yan, M; Wang, S; Sun, S; Sun, Z.** 2009. Shielding effect rule of thermal fatigue crack net and calculating method of stress intensity factor of main crack, Journal of Mechanical Engineering 45(12): 279-283 (In Chinese).
http://dx.doi.org/10.3901/JME.2009.12.279.

4. **Haddar, N; Fissolo, A; Maillot, V.** 2005. Thermal fatigue crack networks: an computational study, International Journal of Solids and Structure 42(2): 771-788.
http://dx.doi.org/10.1016/j.ijsolstr.2004.06.033.

5. **Kamaya, M; Taheri, S.** 2008. A study on the evolution of crack networks under thermal fatigue loading, Nuclear Engineering and Design 238(9): 2147-2154.
http://dx.doi.org/10.1016/j.nucengdes.2008.01.017.

6. **Tsang, D; Oyadiji, S; Leung, A.** 2003. Multiple penny-shaped cracks interaction in a finite body and their effect on stress intensity factor, Engineering Fracture Mechanics 70(15): 2199-2214.
http://dx.doi.org/10.1016/S0013-7944(02)00206-0.

7. **Kamaya, M.** 2008. Influence of the interaction on stress intensity factor of semielliptical surface cracks, Journal of Pressure Vessel Technology Transaction of the ASME 130(1): 011406.
http://dx.doi.org/10.1115/1.2826424.

8. **Kamaya, M.** 2008. Growth evolution of multiple interaction surface cracks. Part II: Growth evaluation of parallel cracks, Engineering Fracture Mechanics 75(6): 1350-1366.
http://dx.doi.org/10.1016/j.engfracmech.2007.07.014.

9. **Lam, K; Phua, S.** 1991. Multiple crack interaction and its effect on stress intensity factor, Engineering Fracture Mechanics 40(3): 585-592.
http://dx.doi.org/10.1016/0013-7944(91)90152-Q.

10. **Bouiadjra, B; Benguediab, M; Elmeguenni,M; Belhouari, M; Serier, B; Aziz, M.** 2008. Analysis of the effect of micro-crack on the plastic strain ahead of main crack in aluminium alloy 2024 T3, Computational Materials Science 42(1): 100-106.
http://dx.doi.org/10.1016/j.commatsci.2007.06.012.

11. **Raju, I.S; Newman, J.C.** 1979. Stress intensity factor for a wide range of semi-elliptical surface cracks in finite-thickness plates, Engineering Fracture Mechanics 11(4): 817-829.
http://dx.doi.org/10.1016/0013-7944(79)90139-5.

12. **Qing, H; Yang, W.** 2006. Characterization of strongly interacted multiple cracks in an infinite plate, Theoretical and Applied Fracture Mechanics 46(3): 209-216.
http://dx.doi.org/10.1016/j.tafmec.2006.10.001.

Xiaosong Wang, Weizheng Zhang

EVOLUTION AND INTERACTION OF SURFACE
CRACKS UNDER THERMAL SHOCK LOAD

S u m m a r y

This paper investigates the evolution and interaction of thermal shock cracks through experiment and FEM simulation. Thermal shock test is conducted to study the thermal cracks evolution behaviour and the FEM simulation is proposed to study the temperature, thermal stress, and SIF distribution between thermal cracks. Results show that the thermal cracks nucleate on the specimen surface and finally form in stable thermal crack network. Large temperature and thermal stress gradient would occur in the cooling process. Parallel and coplanar cracks both reflects quite weak interactions in crack shielding and enhancing effect respectively. All the simulation results could prove the evolution behaviour of thermal cracks obtained in the thermal shock test.